Natural Resources, 2024, 15, 28-50
https://www.scirp.org/journal/nr
ISSN Online: 2158-7086
ISSN Print: 2158-706X

Characteristics of Gold and Its Mineralization Style in the Boulon Djounga Eastern Perimeter of Liptako Mining Company (Central Southwestern Niger)

Gambo Ranaou Noura[1*], Kamayé Tourba[1], Karimou Dia Hantchi[2*], Bouba Hassane[1], Moussa Konaté[1]

[1]Department of Geology, Faculty of Science and Techniques, Abdou Moumouni University, Niamey, Niger
[2]Department of Geology, Faculty of Science and Techniques, Dan Dicko Dankoulodo University, Maradi, Niger
Email: *nouragambo828@gmail.com, diah.uddkm@gmail.com

How to cite this paper: Noura, G.R., Tourba, K., Hantchi, K.D., Hassane, B. and Konaté, M. (2024) Characteristics of Gold and Its Mineralization Style in the Boulon Djounga Eastern Perimeter of Liptako Mining Company (Central Southwestern Niger). *Natural Resources*, **15**, 28-50.
https://doi.org/10.4236/nr.2024.151003

Received: December 19, 2023
Accepted: January 23, 2024
Published: January 26, 2024

Abstract

The Boulon Djounga eastern perimeter is part of the Tiawa operating permit of the *Société des Mines du Liptako* (SML), located in the central southwestern part of Liptako (Niger). In this study, we used field data, Reverse Circulation (RC) surveys and chemical analyzes of gold to determine the characteristics of gold and its mineralization style. The eastern perimeter of Boulon Djounga is represented by a succession of metabasalts and metasediments both intersected by intrusions of quartz and dolerite dykes, and covered by sandstone and clayey rocks. Gold is present in low contents (0.00 - 0.30 ppm) in the sedimentary cover and in medium (0.30 - 1.00 ppm) or high contents (1.00 - 4.534 ppm) in the metasediments, and in the gray quartz veins and locally in the volcanics. It exists in a disseminated state or in a concentrated state in the surrounding areas in the form of discrete grains associated with sulphurous minerals (pyrite: FeS_2, chalcopyrite: $CuFeS_2$ or arsenopyrite: FeAsS). The presence of gold in the quartz veins, and the NE-SW and NW-SE orientations of the ore bodies suggest that the eastern Boulon Djounga gold mineralization would be established during a late magmatic extensive phase.

Keywords

Liptako, Gold Mineralization, Metasediments-Volcanics, Quartz Veins, Sulphurous Minerals, Niger

1. Introduction

The synoptic study of gold mineralization in West Africa has made it possible, on the one hand, to associate the occurrences of gold with rocks belonging to Paleoproterozoic greenstone belts dated to approximately 2.1 Ga [1] and, on the other hand, to consider them as being the consequences of the Eburnean orogeny [2] [3] [4] [5]. Classes of deposit indices, increasingly numerous in the metasedimentary basins of the West African Craton, are related to the deformed and metamorphosed formations in the greenschist facies [6]. According to Castaing *et al.* [7], more than 80% of gold extracted from the West African subsoil comes from rocks forming greenstone belts. Thus, numerous deposits, associated with greenstone belts or metasedimentary basins, have been recognized in Ghana [8] [9] [10] [11], Burkina Faso [2] [12], Mali [6] [13] [14], Senegal [15], Ivory Coast [16] [17] and Morocco [18] [19].

The characteristics of orogenic type deposits are numerous and are defined in terms of structural and lithological controls, as well as in terms of mineral paragenesis. However, supergene alteration of orogenic deposits is among the most important controlling agents and/or major players in the genesis of non-orogenic gold concentrations in time and space [6]. Paleoplacers (non-orogenic deposits of alluvial types) are the most widespread representatives of this type of deposits reported in Ghana [11] [20], Mauritania [21], Ivory Coast [22], Burkina Faso [23] [24] and Mali [25] [26].

In Niger, although the two types of deposits (orogenic and non-orogenic) have been recognized in the Liptako base and in the sedimentary basins through gold panning and industrial gold exploitation activities by the *Société des Mines du Liptako* (SML), research work on gold mineralization still remains very limited. Generally speaking, the available bibliographic data consists mainly of technical reports [27]-[32] and does not provide broad visibility regarding the structural characteristics, lithological and paragenetic of the gold deposits revealed.

Indeed, through its mining complex, the *Société des Mines du Liptako* has been mining gold since October 2004. In order to maintain the level of production, this company looked for additional deposits in 2016. Thus, RC type mining survey work was undertaken in the eastern perimeter of Boulon Djounga to develop the deposit highlighted by previous work [32]. To do this, samples of drill cuttings were collected, then thin and polished sections were made for petrography and microscopy analysis of the mineralization, in addition to the determination of gold contents [33]. All the work undertaken in the sector [29] [30] [31] [32] [33] recommends that most of the exploited deposits appear in the heart of hinge folds oriented towards the south. It is also shown that in the Samira deposit, the ore bodies draw lenticular contours [31], which dipped varying from 40 to 45°towards the ENE [31], or towards the NE [32]. Furthermore, petrographic and mineralogical studies do not make a significant contribution to models of the empirical relationships that control the distribution of gold mineralization, despite the importance of such studies in the interpretation of styles of gold mineralization [12] [18]. The objective of this study is to determine the geological characteristics of the gold deposits of the eastern Boulon Djounga deposit, in terms of the lithogeochemical and mineralogical aspects of this sector.

2. Geological Setting

2.1. Liptako Geological Setting

The *Société des Mines du Liptako* (SML), commonly called Samira, is located in the southwestern Center of Nigerien Liptako (**Figure 1**; [34]). The Nigerien Liptako corresponds to the northeastern border of the Baoulé-Mossi domain belonging to the Léo-Man Dorsal [35]. The basement formations of this Birimian domain were granitized, metamorphosed and stabilized between 1.8 Ga and 1.6 Ga [36] [37].

The basement of the Nigerien Liptako is made up of two geological groups, notably the greenstone belts of Gorouol, Diagorou-Darbani and Sirba, intersected by the granitoid plutons of Téra-Ayorou, Dargol-Gothèye and Torodi (**Figure 2**; [38]). The Liptako greenstone belts are made up of meta-volcanosediments, metasediments, metabasites and meta-ultrabasites [28] [39]-[48]. Conversely, granitoid plutons are made up of calc-alkaline rocks including a series of Tonalites, Trondhjemites, Granodiorites (TTG) and acidic to intermediate rocks of various nature including diorites, syenites, granites and dacites [49] [50] [51]. All of the Birimian rocks are cross-cutted by dykes of pegmatites, quartzo-feldspars-rich veins and dolerite dykes [40] [48]; all these rocks are being covered by sedimentary formations of various ages [52] [53] [54] [55]. It is accepted that in

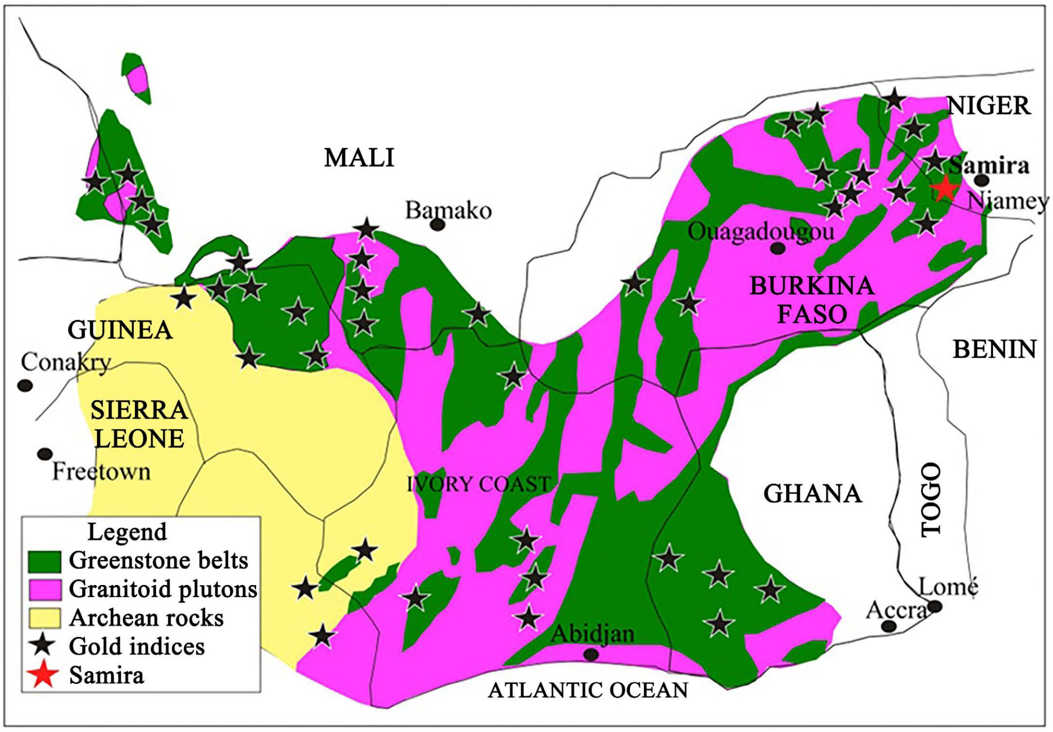

Figure 1. General geological map showing the main gold showings of West Africa and the study area: Samira (Modified from [34]). The red star represents the Samira Gold mine domain.

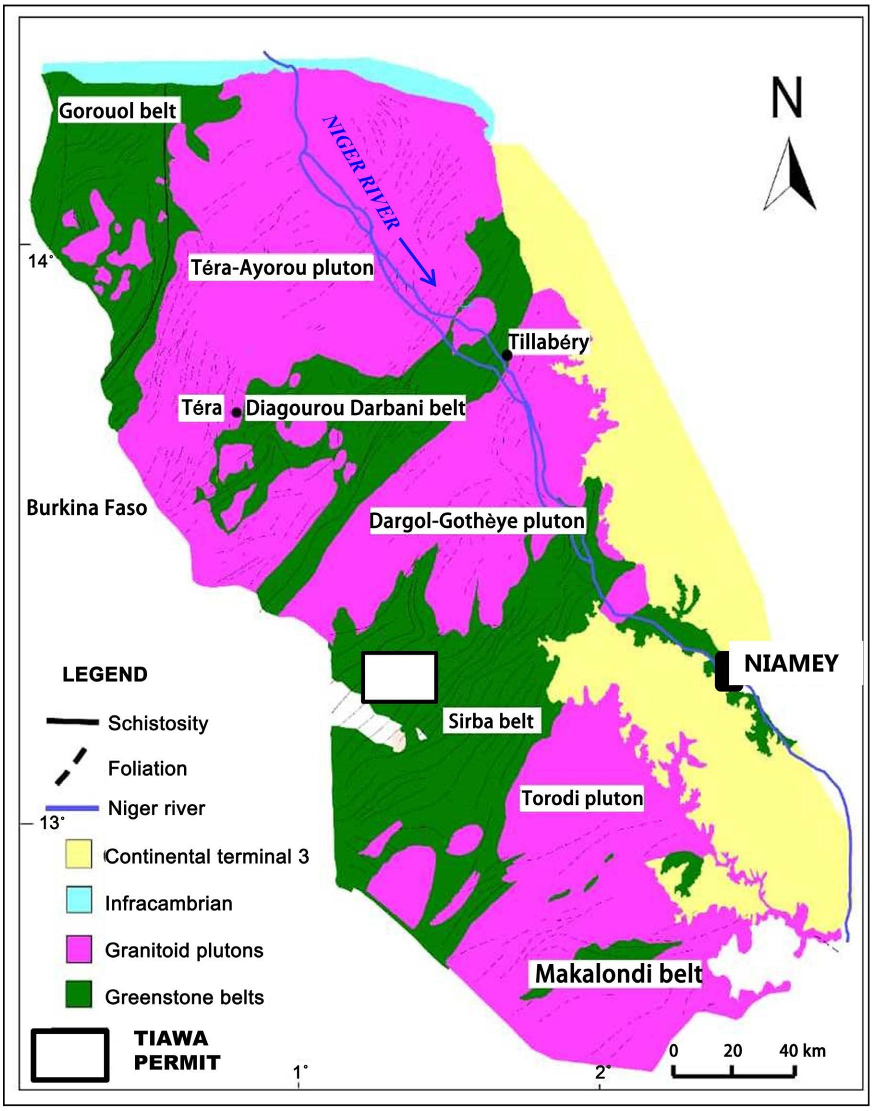

Figure 2. Simplified geological map of the Niger Liptako (Modified from [38]). The Sirba greenstone belt is the host formation of the Samira Tiawa permit.

the Léo-Man ridge, most of the gold showings discovered are located in the greenstone belts of the Baoulé-Mossi domain up to including the Nigerien Liptako [34] [56], as opposed to the archaean domain of Kenema-Man which presents few clues (**Figure 1**).

2.2. Eastern Boulon Djounga Geological Setting

The eastern Boulon Djounga perimeter is located in the Sirba greenstone belt, the geological formations hosting the Tiawa permit of the Samira mine (**Figure 2**). The Sirba greenstone belt is composed of metabasites (basalts, dolerites and gabbros), metasediments (schists, siltstones, pelites, quartzites, greywackes, conglomerates) and locally by plutonic magmatic rocks (granites, granodiorites, diorites, rhyodacites, rhyolites and granophyres) [28] [39] [57]. These rocks are metamorphosed in greenschist facies in the axial zone of the greenstone belts rising to amphibolite facies in the vicinity of plutons with local partial melting [57].

In the Tiawa exploitation permit and particularly in the eastern perimeter of Boulon Djounga, the area is formed of mafic volcanics with intercalations of metasediments and volcanosediments (**Figure 3**). These formations are intersected, in places, by gabbro and dolerite veins and dykes as well as small granitoid and felsic plutons [31] [58] [59].

Geological mapping work and core surveys, as well as interpretations of *Remote Sensing* and *Airborne geophysics* data, have shown that the gold deposits of the *Société des Mines du Liptako* are located on a distinct horizon of metasediments, commonly called the "Samira Sedimentary Sequence" [29] [30] [31] [32] [58] [59]. This sequence is subdivided into four (4) distinct groups from the grain size and the nature of the composite material. These include weakly metamorphosed interbedded sandstones and greywackes, fragmentary metasediments, interbedded and laminated metavolcanics, and both granoclassified and interbedded metasediments (**Figure 4**).

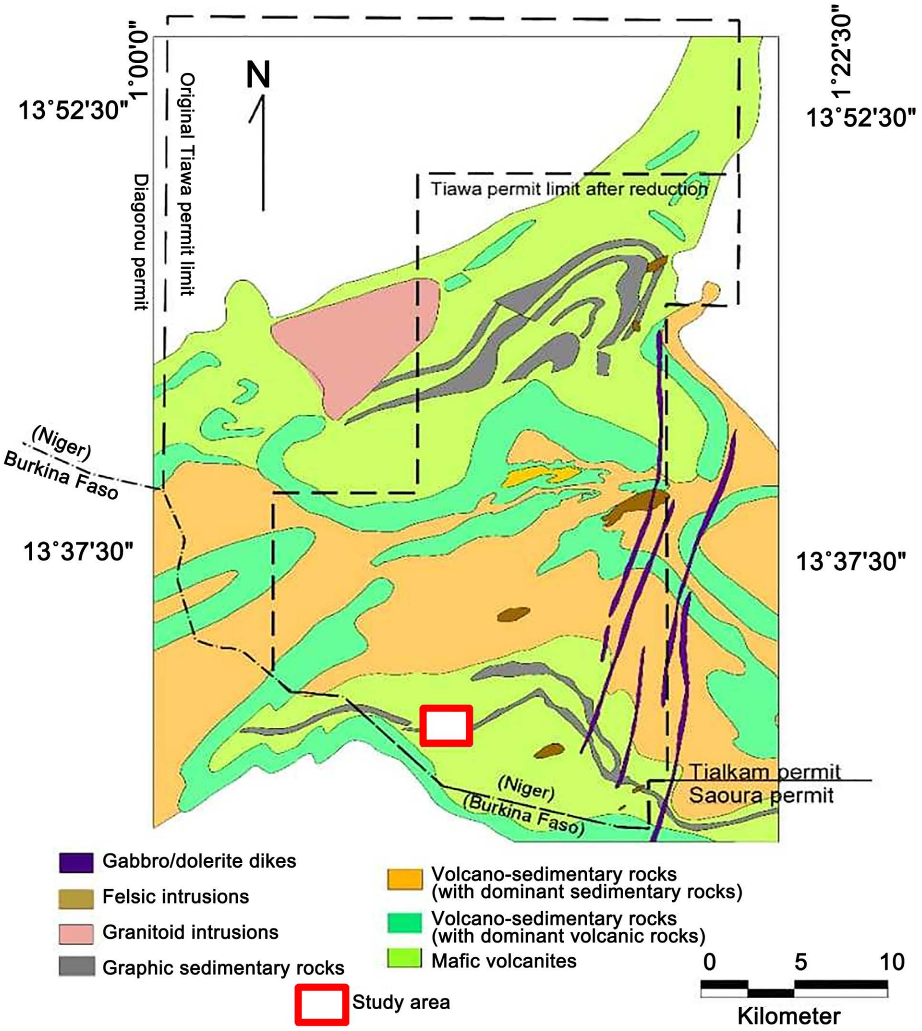

Figure 3. Geological map of the Tiawa Permit (SML [32]). The red rectangle represents the study area.

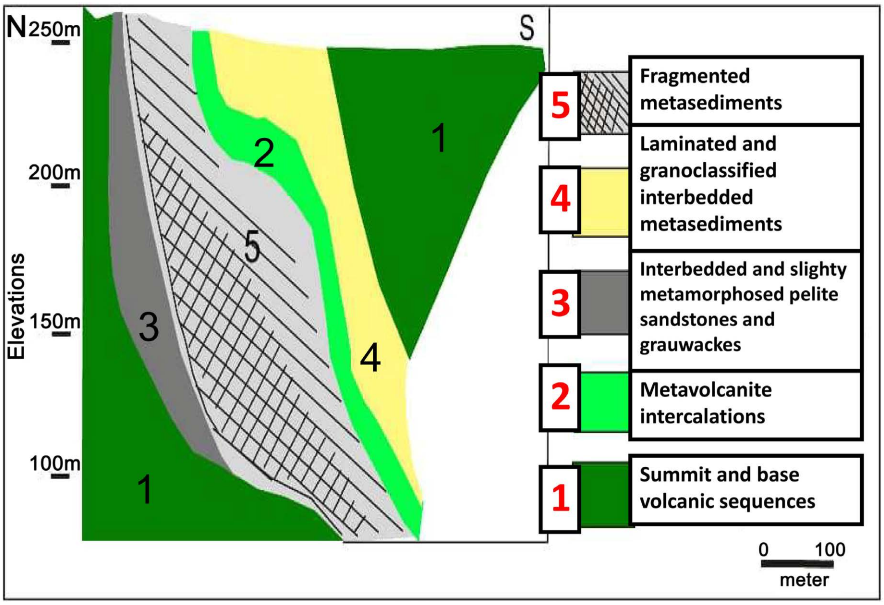

Figure 4. Simplified geological diagram of the Samira sedimentary sequence (SML [32] modified).

3. Material and Methods

The cuttings were collected during twelve (12) RC surveys carried out in the prospect of eastern Boulon Djounga. The RC surveys were distributed into three (3) cross sections (CT001, CT002, CT003) oriented N-S. Each cross section has four (4) boreholes, spaced of 100 m (**Figure 5**).

The soundings, with a depth varying from 90 m to 97 m, bear the names 16BJE000 to signify a BJE drilling from 2016 and serial numbers (here: 001 to 012). For each excavated material from a one-meter borehole, the excavated raw materials are collected in a white plastic bag, which is attached to the cyclone spillway. The dried and weighed spoil is then dumped into a divider so that it is homogenized and divided into parts, which pass through weirs of the divider and collected in two trommels (iron boxes). The aliquots (3 to 5 kg) of cuttings from the trommels are placed in plastics for chemical analyses. Likewise, we take a quantity which we wash and sieve. Refusals are entered into a box for field description.

The series of samples collected is the subject of operations to describe the raw debris and laboratory works. The description of the raw cuttings makes it possible to determine the petrography, the alteration profile of the rocks and that oxidation of sulphides at each hole. This is done according to three parameters depending on the images of the same petrographic composition, including major lithology, abundance of certain minerals, and laterite boundary. The laboratory work consisted of the preparation of thin sections, their observation under an optical microscope with transmitted light and the chemical determination of gold at the *SGS Burkina SA Laboratory* (Ouagadougou, Burkina Faso). Lithological logs and the vertical and lateral extents of the ore bodies were designed

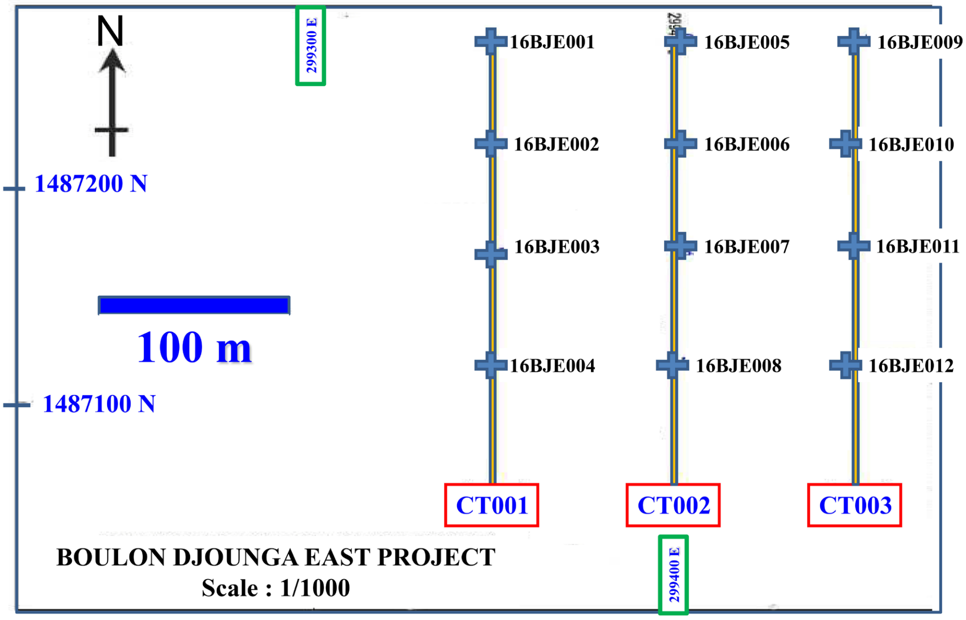

Figure 5. Location of Reverse Circulation (RC) surveys in the eastern sector of Boulon Djounga (SML [33] modified). The cross sections, with the 12 boreholes (16BJE000), spaced of 100 m, are indicated as CT001, CT002 and CT003.

and correlated on the three (3) cross sections (Figure 5) by insertion of petrographic data and chemical assay results.

4. Results

4.1. Petrography

The macroscopic description of RC drilling cuttings and spoils, the lithological logs and thin sections in polarized light analyzed demonstrates that the study perimeter is made up of several lithologies, listed as follows from top to base:

Laterites

This is the summit level made up of the armor and the carapace. The two sub-levels are both composed of a mixture of ferruginous sandstone and argillaceous sandstone of brick-red color, of massive structure and rich in hematite, iron nodules, goethite and gibbsite (Figure 6(a) and Figure 6(b)). The armor and the carapace have variable thicknesses depending on the geomorphological profile. The thicknesses highlighted on the three cross sections (CT001, CT002 and CT003) are between 0 and 20 m (Figures 7-9). The different structures observed in the upper part of the ferruginous zone of the lateritic regolith are massive pisolites fabrics pisolites and iron nodules or vesicles.

Spotted clays

They are a massive level presenting several colors (red, brown or yellow spotted with white). This level corresponds to the clay layer presenting a shade of color between kaolin, hematite and limonite (Figure 6(a) and Figure 6(b)). Its thickness according to the three cross sections is between 1 m and 2 m (Figures 7-9).

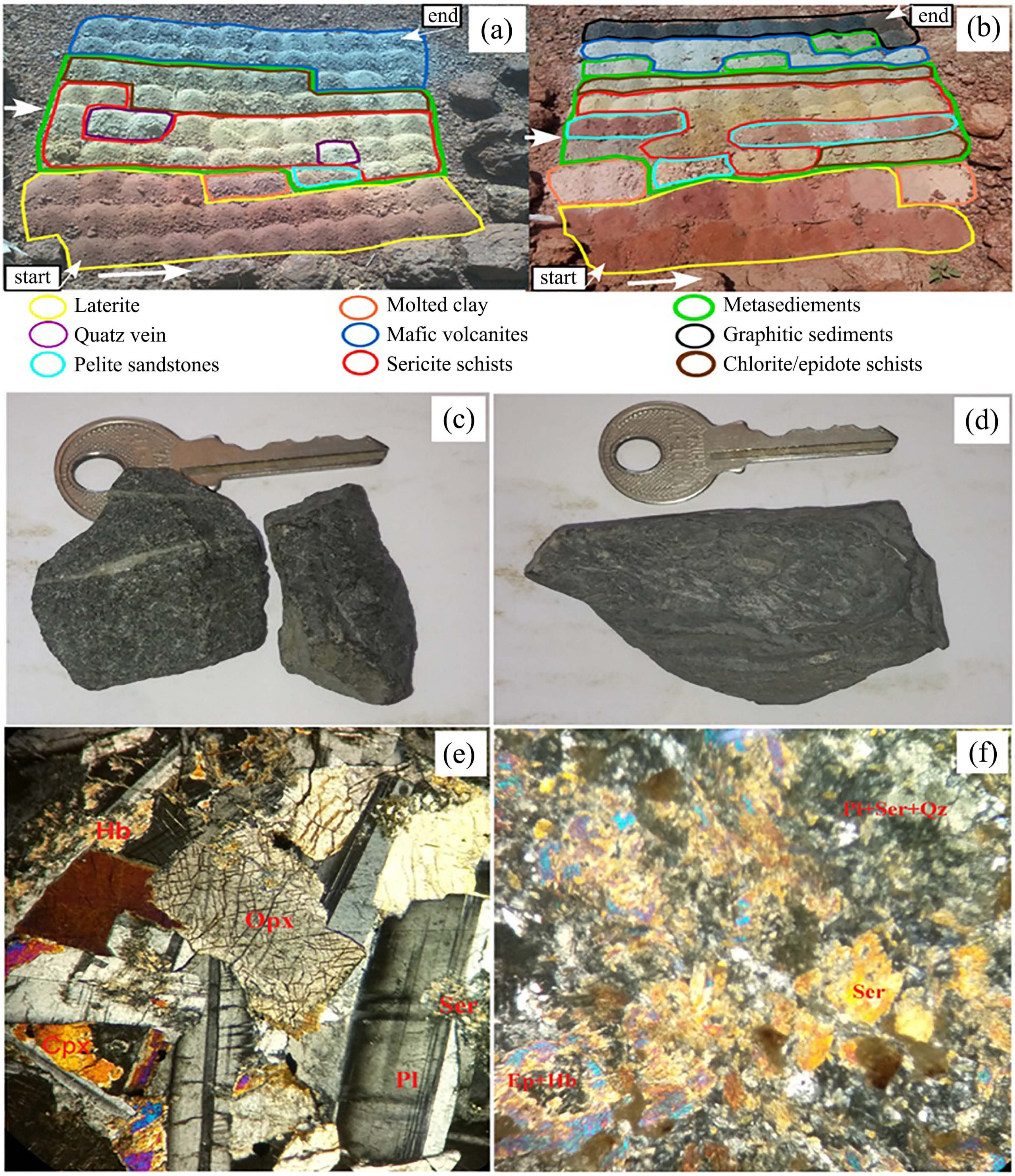

Figure 6. (a) and (b) description of the cuttings, (c) samples of dolerite dykes, (d) samples of metabasalt ((e) (f)) photomicrographs of the dolerite and metabasalt dykes. Ser: sericite; Opx: orthopyroxene; Cpx: clininopyroxene; Pl: plagioclase, Ep: epidote, Qz: quartz, Hb: hornblende.

Metasediments

They are essentially schistose and present several colors (gray, yellowish gray, greenish gray, green, brown and beige). Among the minerals observed, we could

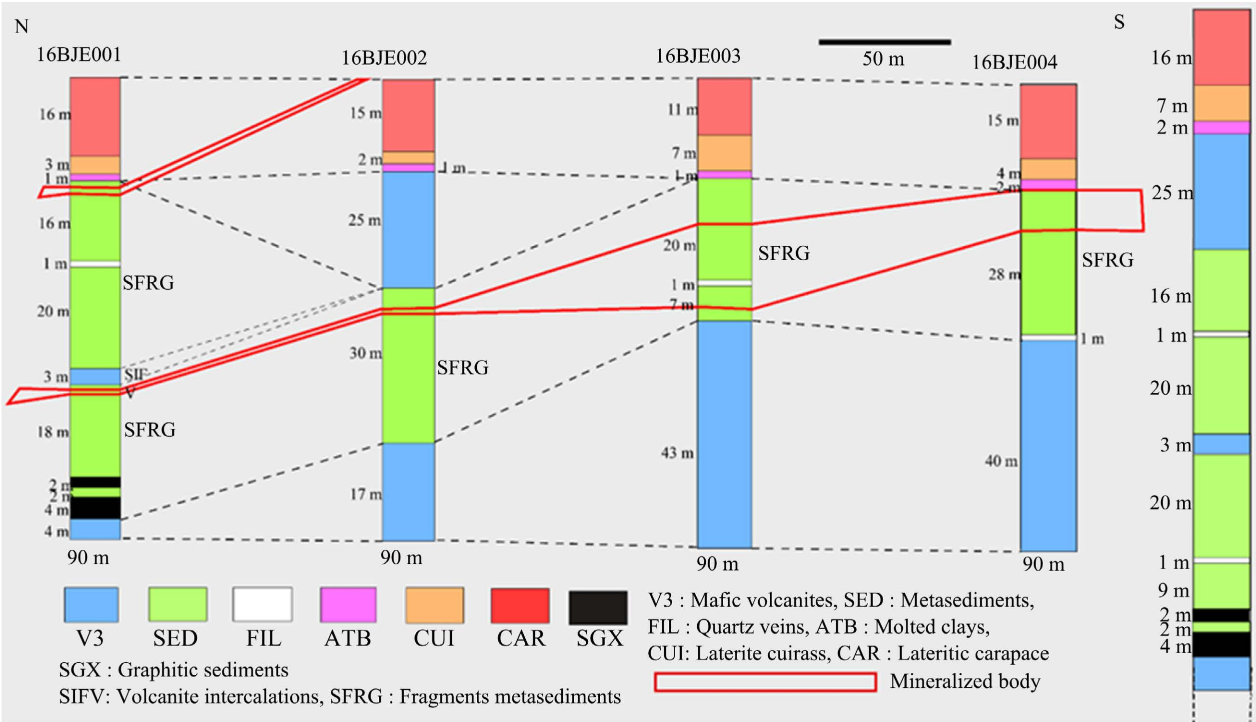

Figure 7. Correlation of the lithological logs of the CT001 cross section and delineation of the ore body within the metasediments. The red rectangle represents the mineralized body.

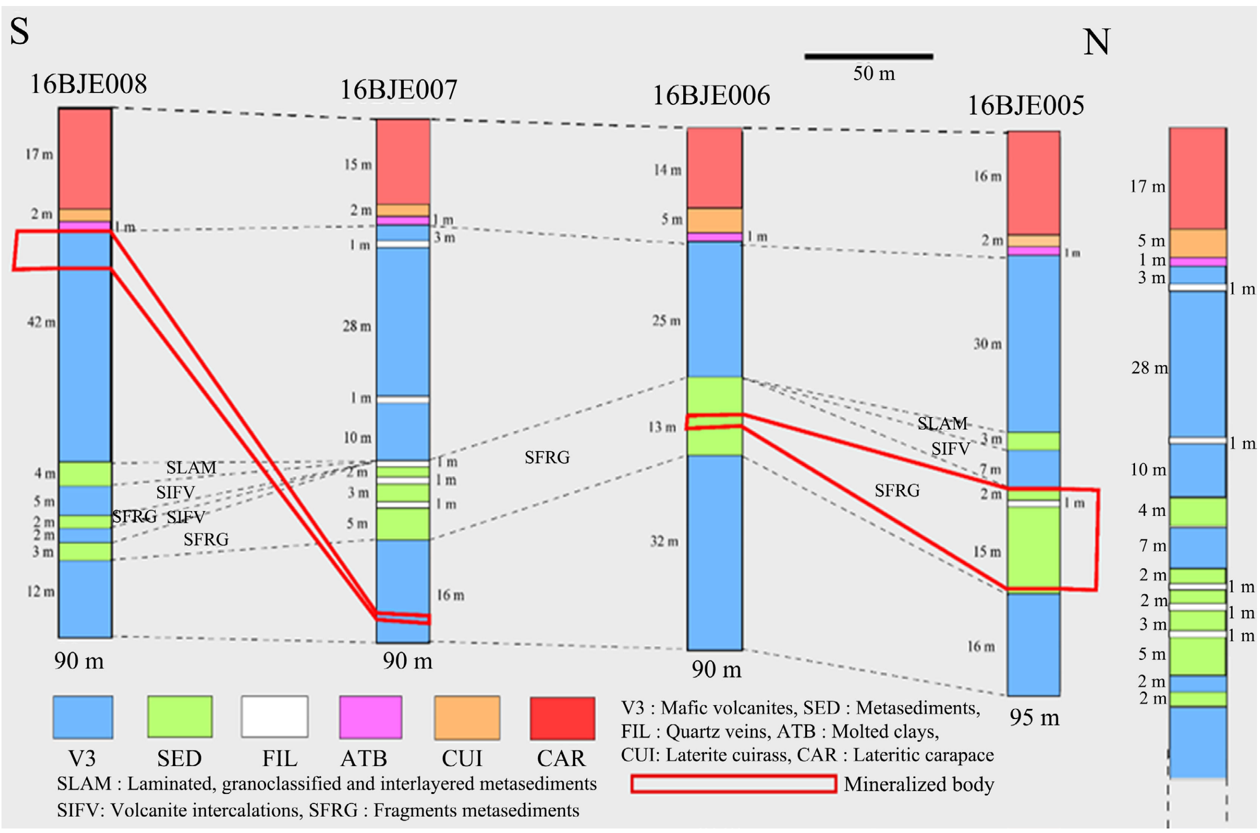

Figure 8. Correlations of lithological logs of cross section CT002 and delineation of the ore body within metasediments and mafic volcanics. The red rectangle represents the mineralized body.

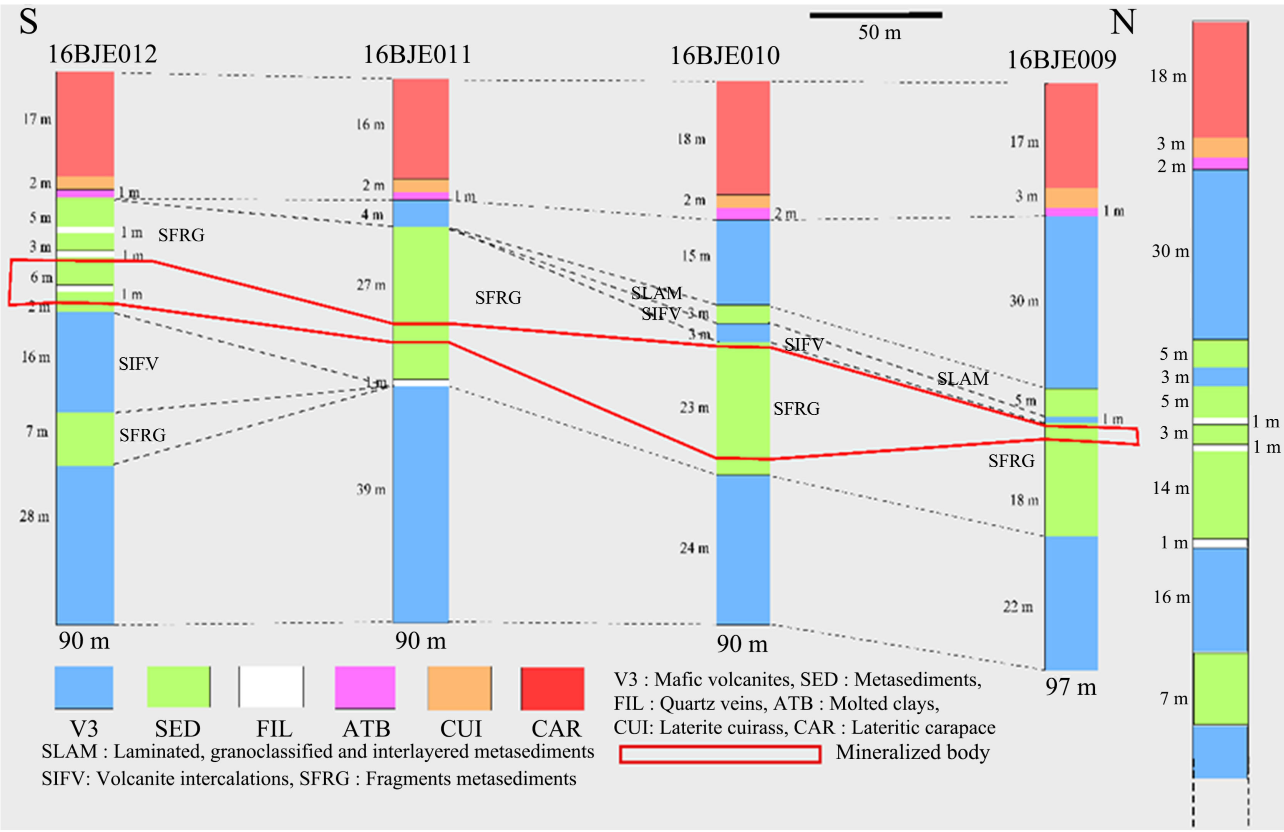

Figure 9. Lithological log correlations of cross section CT003 and delineation of the ore body within the metasediments. The red rectangle represents the mineralized body.

distinguish quartz, chlorite, sericite and pyrite. The description of the cuttings shows that they correspond to chlorite, sericite or epidote schists, greywackes, sandstone pelites or gresopelites (Figure 6(a) and Figure 6(b)). The schistosity is well marked in the shales and crude in the sandstone pelites, sandstones and greywackes. The levels occur locally in intercalation with mafic volcanics. The metasediments occur at depths between 20 m and 86 m (Figures 7-9).

Quartz veins

They are white or gray in color and are characterized by a vein structure (Figure 6(a) and Figure 6(b)). They cross-cut the metasediments and volcanics over thicknesses of approximately 1 m (Figures 7-9).

Graphite-bearing sediments

They have a thickness of 6 m, a black color and a schistose structure (Figure 6(b)). Alternating with meta-sediments, graphite-bearing sediments were observed only in the borehole 16BJE000. They correspond to the sedimentary horizon bearing the Samira gold mineralization.

Mafic volcanites

They have a black or green tint and a massive or schist structure in places (Figure 6(a), Figure 6(b) and Figure 6(d)). The black color characterizes healthy massive rocks, in which white quartz and pyrite are observed. The other colors are observed on altered volcanics, rich in chlorite and/or epidote. When the latter are schist, they represent chloritoschist/epidote schists. Microscopic observation of a thin section of a volcanic sample taken at 40 m in borehole BJE009 shows a mineralogical composition represented by plagioclase, amphibole, epidote, sericite and quartz (**Figure 6(d)** and **Figure 6(f)**). This mineralogical composition is typical of a basalt. A sample of grey dolerite dyke with massive structure, cutting the volcanics at 45 m in borehole 16BJE008, indicates that it is made up of pyroxene, plagioclase, sericite and hornblende (**Figure 6(e)** and **Figure 6(f)**). The lack of schistosity on the dolerite dykes indicates that they correspond to Birimian late-magmatic events.

The petrographic results show that the lithologies of the Boulon Djounga Est perimeter have undergone hydrothermal and meteoric alteration processes. The evolution of the mineral phases shows primary minerals (pyroxene and plagioclase) transformed on the edges into hornblende, chlorite or epidote and in the center into sericite, during hydrothermal alteration. Meteoric alteration affected the rocks in the form of ferralitic and silico-aluminous processes and consisted respectively of the hydrolysis of ferromagnesian minerals (amphibole, pyroxene, chlorite) and plagioclase.

4.2. Chemical Assays of Gold

The gold chemical assay results are given in ppm for each 1 m pass of drilling progress and are recorded in **Table 1**. The grades obtained on the twelve boreholes vary from 0 to 4.534 ppm. The average grades (X) per survey vary from 0.032 to 1 ppm and the average grade for all 12 surveys is 0.14 ppm.

Table 1. Gold chemical assay result in ppm. The interesting contents have been indicated in bold in the table. CNR designates "cuttings not recovered" during the survey. Σ and X are respectively the sum and the average of the ppm contents obtained at each borehole.

Chemical analysis results per one meter pass (Au in ppm)												
Depth (m)	*16BJE001*	*16BJE002*	*16BJE003*	*16BJE004*	*16BJE005*	*16BJE006*	*16BJE007*	*16BJE008*	*16BJE009*	*16BJE010*	*16BJE011*	*16BJE012*
1	CNR	CNR	0.007	CNR	0.021	0.002	CNR	CNR	0.008	0.009	0.017	0.016
2	CNR	0.006	0.007	0.002	0.002	0.006	0.014	0.002	0.006	0.018	0.023	0.008
3	0.026	0.006	0.007	0.002	0.009	0.002	0.010	0.002	0.022	0.011	0.002	0.010
4	0.012	0.005	0.008	0.002	0.006	0.002	0.018	0.076	0.022	0.015	0.007	0.009
5	0.002	0.006	0.008	0.008	0.013	0.011	0.025	0.031	0.011	0.013	0.002	0.094
6	0.006	0.006	0.011	0.008	0.014	0.002	0.036	0.013	0.020	0.035	0.033	0.008
7	0.006	0.012	0.017	0.030	0.022	0.006	0.026	0.041	0.018	0.039	0.031	0.011
8	0.010	0.017	0.019	0.020	0.062	0.006	0.057	0.007	0.013	0.068	0.052	0.041
9	0.021	0.035	0.032	0.017	0.040	0.009	0.019	0.002	0.023	0.022	0.042	0.042
10	0.013	0.024	0.024	0.011	0.030	0.011	0.047	0.068	0.016	0.012	0.048	0.036
11	0.014	0.043	0.022	0.006	0.030	0.012	0.056	0.009	0.026	0.027	0.045	0.036
12	0.022	0.033	0.021	0.008	0.088	0.011	0.034	0.030	0.039	0.029	0.044	0.037

Continued

13	0.024	0.029	0.030	0.023	0.014	0.014	0.049	0.002	0.055	0.050	0.024	0.020
14	0.042	0.035	0.032	0.031	0.020	0.012	0.062	0.002	0.054	0.030	0.026	0.028
15	0.056	0.047	0.048	0.056	0.020	0.013	0.040	0.022	0.039	0.025	0.020	0.020
16	0.077	0.029	0.055	0.041	0.008	0022	0.031	0.027	0.022	0.031	0.027	0.016
17	0.055	0.019	0.035	0.042	0.040	0.027	0.057	0.046	0.022	0.029	0.026	0.024
18	0.128	0.038	0.059	0.061	0.025	0.014	0.029	0.028	0.051	0.032	0.041	0.030
19	0.042	0.021	**0.367**	0.065	0.021	0.019	0.018	0.049	0.014	0.036	0.067	0.043
20	0.028	0.034	0.035	0.102	0.013	0.008	0.035	**0.428**	0.012	0.037	0.030	0.025
21	0.128	0.050	0.062	**4.534**	0.008	0.007	0.020	**4.432**	0.008	0.035	0.036	0.037
22	**0.595**	0.023	0.016	0.198	0.006	0.018	0.118	**0.512**	0.008	0.018	0.058	0.013
23	0.236	0.010	0.012	0.076	0.008	0.041	0.169	0.078	0.009	0.021	0.011	0.061
24	0.260	0.013	0.013	0.027	0.016	0.022	0.197	0.056	0.010	0.026	0.030	0.020
25	0.036	0.011	0.026	0.015	0.014	0.006	0.270	0.053	0.010	0.016	0.066	0.062
26	0.078	0.017	0.174	**0.436**	0.002	0.008	0.294	**0.974**	0.006	0.012	0.213	0.020
27	0.042	0.007	0.014	0.233	0.006	0.006	**0.345**	0.108	0.018	0.011	0.015	0.007
28	0.034	0.008	**0.825**	**0.639**	0.002	0.008	0.139	0.101	0.017	0.006	0.050	0.007
29	0.014	0.002	0.103	0.097	0.002	0.002	0.015	0.092	0.006	0.014	0.054	0.022
30	0.080	0.012	0.018	0.011	0.008	0.020	0.073	0.111	0.002	0.017	0.028	0.189
31	0.009	0.005	0.021	0.062	0.002	0.006	0.273	0.021	0.008	0.006	0.028	**0.343**
32	0.020	0.007	0.015	0.052	0.002	0.031	**0.397**	0.008	0.002	0.002	0.010	**0.393**
33	0.007	0.012	0.200	0.050	0.011	0.002	0.099	0.012	0.002	0.009	0.072	0.029
34	0.016	0.013	0.107	0.039	0.006	0.002	0.062	0.163	0.002	0.023	0.015	0.050
35	0.002	0.011	0.091	0.034	0.014	0.002	0.028	0.020	0.005	0.008	0.014	**0.589**
36	0.002	0.010	0.193	0.006	0.006	0.002	0.059	0.013	0.013	0.025	0.017	0.202
37	0.002	0.008	0.162	0.002	0.013	0.010	0.083	0.024	0.006	0.026	0.033	0.057
38	0.002	0.009	0.180	0.002	0.013	0.020	0.051	0.011	0.002	0.024	0.085	0.005
39	0.002	0.024	0.125	0.006	0.004	0.002	0.020	0.021	0.009	0.042	0.038	0.049
40	0.010	0.015	0.293	0.006	0.050	0.002	0.076	0.013	0.002	0.021	0.119	0.093
41	0.047	0.015	**1.354**	0.007	0.011	0.002	0.018	0.041	0.002	0.024	0.165	0.329
42	0.007	0.010	**1.324**	0.002	0.002	0.008	0.031	0.010	0.002	0.029	**0.307**	0.066
43	0.002	0.002	**0.321**	0.007	0.007	0.002	0.004	0.169	0.002	0.002	**0.424**	0.053
44	0.002	0.006	0.076	0.013	0.002	0.006	0.007	0.025	0.006	0.153	0.057	0.020
45	0.002	0.054	0.064	0.007	0.002	0.018	0.084	0.019	0.021	0.237	0.032	0.013
46	0.002	**1.102**	0.079	0.002	0.002	0.027	0.042	0.006	0.002	**0.303**	0.035	0.038
47	0.012	**0.581**	0.052	0.002	0.002	0.009	0.061	0.014	0.002	**0.740**	0.108	0.012
48	0.006	0.238	0.029	0.007	0.002	0.006	0.007	0.014	0.022	**0.553**	0.195	0.063
49	0.024	0.023	0.021	0.002	0.002	0.002	0.178	0.008	0.035	**0.342**	0.044	0.045
50	0.014	0.116	0.012	0.002	0.002	0.007	0.279	0.002	0.029	0.073	0.013	0.047

Continued

51	0.024	0.067	0.012	0.002	0.012	0.002	0.033	0.002	0.057	0.050	0.007	0.013
52	0.050	0.039	0.011	0.010	0.002	**0.855**	0.013	0.008	0.055	0.068	0.010	0.008
53	0.032	0.016	0.007	0.014	0.029	**0.416**	0.037	0.013	0.016	0.034	0.036	0.032
54	0.036	0.164	0.015	0.023	0.030	0.035	0.070	0.019	0.028	0.016	0.023	0.048
55	0.009	**0.394**	0.008	0.021	0.016	0.025	0.035	0.031	0.202	0.018	0.024	0.041
56	0.002	0.265	0.002	0.036	0.018	0.014	0.024	0.065	**2.108**	0.027	0.012	0.008
57	0.002	0.152	0.002	0.033	0.007	0.011	0.024	0.036	**1.184**	0.030	0.011	0.002
58	0.002	0.085	0.002	0.045	0.007	0.016	0.034	0.035	0.292	0.018	0.015	0.002
59	0.002	0.016	0.002	0.022	0.002	0.042	0.032	0.055	0.026	0.025	0.009	0.004
60	0.013	0.090	0.002	0.011	0.009	0.023	0.015	0.031	0.079	0.012	0.008	0.050
61	0.026	0.012	0.002	0.016	0.043	0.054	0.018	0.046	0.046	**0.654**	0.002	0.002
62	0.006	0.015	0.002	0.034	0.012	0.024	0.012	0.026	0.069	0.040	0.002	0.002
63	**1.406**	0.026	0.002	0.035	0.011	0.018	0.064	0.013	0.115	0.041	0.009	0.007
64	**0.676**	0.013	0.002	0.046	**0.972**	0.064	0.045	0.006	0.079	0.064	0.005	0.002
65	0.018	0.014	0.006	0.015	0.081	0.061	0.019	0.042	0.096	0.045	0.002	0.008
66	0.104	0.012	0.007	0.011	**0.301**	0.148	0.002	0.028	0.020	0.020	0.016	0.023
67	0.060	0.014	0.006	0.021	**2.827**	0.107	0.021	0.023	0.068	0.032	0.011	0.015
68	0.002	0.014	0.007	0.060	0.079	0.011	0.084	0.004	0.095	0.025	0.020	0.006
69	0.028	0.008	0.002	0.019	0.046	0.007	0.036	0.017	0.033	0.017	0.006	0.010
70	0.006	0.010	0.002	0.006	**0.780**	0.006	0.042	0.010	0.079	0.038	0.026	0.002
71	0.088	0.048	0.007	0.002	0.294	0.002	0.040	0.002	0.041	0.005	0.024	0.002
72	0.094	0.007	0.002	0.007	0.067	0.002	0.025	0.010	0.129	0.002	0.011	0.002
73	0.062	0.029	0.002	0.002	0.008	0.020	0.002	0.010	0.169	0.006	0.010	0.002
74	0.045	0.015	0.007	0.002	0.018	0.007	0.002	0.006	0.093	0.002	0.008	0.002
75	0.019	0.017	0.002	0.008	0.012	0.002	0.033	0.010	0.017	0.002	0.006	0.002
76	0.007	0.010	0.002	0.002	0.010	0.011	0.035	0.007	0.009	0.002	0.002	0.006
77	0.016	0.009	0.005	0.006	0.019	0.006	0.016	0.186	0.010	0.002	0.007	0.002
78	0.037	0.002	0.002	0.020	0.021	0.022	0.023	0.017	0.011	0.009	0.025	0.005
79	0.049	0.006	0.002	0.029	**0.884**	0.012	0.022	0.010	0.006	0.002	0.020	0.002
80	0.123	0.002	0.002	0.046	**0.326**	0.010	0.002	0.009	0.011	0.002	0.025	0.008
81	0.031	0.002	0.002	0.002	0.106	0.012	0.007	0.010	0.002	0.002	0.010	0.002
82	0.019	0.009	0.002	0.009	0.065	0.019	0.038	0.008	0.002	0.002	0.018	0.014
83	0.008	0.008	0.002	0.009	0.080	0.098	0.153	0.018	0.002	0.002	0.014	0.017
84	0.008	0.002	0.002	0.007	0.049	0.046	**0.636**	0.024	0.008	0.011	0.019	0.002
85	0.018	0.028	0.002	0.002	0.082	0.028	0.208	0.028	0.002	0.002	0.017	0.002
86	0.019	0.002	0.002	0.002	0.061	0.040	0.090	0.016	0.002	0.006	0.012	0.002
87	0.010	0.002	0.007	0.007	0.038	0.018	0.045	0.008	0.002	0.002	0.006	0.015
88	0.010	0.007	0.002	0.002	0.020	0.023	0.092	0.009	0.008	0.002	0.036	0.002

Continued

89	0.011	0.002	0.002	0.002	0.015	0.053	0.041	0.007	0.006	0.002	0.002	0.002
90	0.007	0.006	0.002	0.002	0.010	0.022	0.071	0.011	0.007	0.025	0.002	0.002
91					0.006				CNR			
92					0.007				0.002			
93					0.009				0.021			
94					0.002				0.007			
95					0.002				0.002			
96									0.008			
97									0.008			
Σ	**5.462**	**4.498**	**6.985**	**7.759**	**8.820**	**2.905**	**6.403**	**8.932**	**6.093**	**4.750**	**3.507**	**3.866**
X	**0.062**	**0.050**	**0.078**	**0.087**	**0.087**	**0.032**	**0.072**	**1.000**	**0.063**	**0.053**	**0.039**	**0.043**

By superimposing these contents on the lithological logs, we notice that low contents (0.00 - 0.30 ppm) are frequently observed in laterite, white quartz veins and mafic volcanics while medium ones (0.30 - 1.00 ppm) and high contents (1.00 - 4.534 ppm) are hosted by metasediments and gray quartz veins, with some interesting passes in the mafic volcanics (**Figures 7-9**).

The highest content (4.534 ppm) was observed in fragment metasediments in 16BJE004 (**Table 1**). In gray quartz veins and mafic volcanics, gold is frequently associated with sulphurous minerals (pyrite: FeS_2, chalcopyrite: $CuFeS_2$ or arsenopyrite: FeAsS). It is found in a disseminated state in the surrounding areas because grains of gold were not observed in the cuttings or in the thin sections.

4.3. Lithological Logs

Correlations of lithological and synthetic logs from three cross sections (CT001, CT002, CT003) show a lithological succession composed of six (6) levels from bottom to top. These are mafic volcanics or metabasalts, graphite sediments, metasediments, variegated spotted clay with lateritic armor and carapace. The metabasalts and metasediments are affected by metric-thick quartz intrusions.

Depending on the grain size and the sedimentary or metamorphic structures present, three units of the Samira sedimentary sequence were identified in the eastern sector of Boulon Djounga. These are laminated, graded and interstratified metasediments, metavolcanic intercalations and fragment metasediments (**Figures 7-9**). The disappearance of certain lithological levels from one survey to another could be due to tectonic deformations that affected the rocks. This can be noticed on the summit volcanics to the south of cross sections CT001 and CT003.

The superposition of the grades obtained on each borehole along the corresponding lithological logs (**Table 1**) made it possible to delimit the vertical and lateral extent of the ore bodies, but also to highlight the lithological control of the gold mineralizations in the eastern perimeter of Boulon Djounga (**Figures**

7-9). The ore bodies are characterized by a low dip on the scale of cross sections and a variable thickness depending on the nature of the surrounding environment.

5. Discussion

The hoarding of gold in Niger in recent decades has made it necessary to take into account and above all a better understanding of the mineralization of the Samira gold prospect (South-West Liptako of Niger). In light of this, more economically viable deposits could be brought into production. This study of an area of great diversity of major structures and geological formations, namely the eastern perimeter of Boulon Djounga, is part of this perspective.

Analyzes of lithological logs (macroscopy of cuttings, thin sections and step-by-step correlations) reveal a lithological sequence formed of mafic volcanics or metabasalts which, topped by graphite sediments, are intruded by metric-scale quartz veins. Then, there are metasediments which, in addition to being affected by quartz intrusions, are laminated, granoclassified and interstratified. The summit part is composed of variegated spotted clays on its wall and roof, armor covered with a lateritic carapace. In agreement with Eggleton [60], this is the part of the lateritic profile showing ribbons of different colors whose red tint corresponds to hematite, the yellow tint to limonite and the white tint or gray with kaolin. The differentiations highlighted in this study are similar to the descriptions made by previous authors [31] [32] [58] [59] in the Tiawa and Saoura exploitation permits of the *Société des mines du Liptako* (SML). Also, just like Gilder [61] demonstrated in his mineralogical study on the physical characteristics of gold in the Samira deposits, the gold appears as discrete grains of size between 1 and 50 µm.

Gold mineralization at Samira is mainly developed in fragmental sediments, particularly those in proximal contact with volcanic intercalations. This is consistent with the conclusions of *Placer Dome Inc.* [31], who put forward the hypothesis that the geological control of the gold mineralizations in the Boulon Djounga would be ensured by volcanics which provide a good barrier impermeable to hydrothermal liquids during the placement of gold. Scattered throughout the surrounding areas, gold mineralization is associated with sulphurous minerals (pyrite, chalcopyrite, arsenopyrite). The same similarity has been reported in certain types of deposits described in Ghana by Leube *et al.* [62] and Oberthur *et al.* [63], who reported that disseminated gold is in metasediments just like quartz veins. Furthermore, the characteristics of these mineralizations (*i.e.*, the dissemination of gold in volcanic rocks and quartz veins) are similar to the metallogenic attributions of types II and IV deposits described by Milési *et al.* [34] and type II mentioned by Milési *et al.* [1] and Mcmahon *et al.* [64].

The very high contents (4.432 ppm and 4.534 ppm), obtained in the metasediments of drilling 16BJE004 and in the volcanics of drilling 16BJE008, indicate that gold also exists in a concentrated state, as was indicated by Béziat *et al.* [2]

in an orogenic deposit in Burkina Faso. In this typical case, for [2], gold occurs in both forms namely disseminated and concentrated. However, it remains that the presence of numerous native gold grains can also be associated with pyrite (FeS_2 (traces Ni, Co, Cu, Ag, Au)), as reported by El-Desoky *et al.* [65] in the granites of the Hamash goldmine (South Eastern Desert of Egypt).

From the presence of gold-bearing quartz veins in the volcanics or metasediments and the analysis of the vertical and lateral extents of the ore bodies (**Figures 7-9**), it appears that the geometry of the deposits indicates a pervasive structural control of the gold mineralization by an extensive phase. These results are in line with those of the work of [6] [65] [66], who point out that gold-rich vein structures are in fact associated with large faults forming a conjugate network in relation to the main shear zones.

In this expectation, the ore bodies which have NE-SW and NW-SE orientations would be compatible with the extension directions of the third phase of deformation D3 responsible for brittle shear and the establishment of gold mineralizations in the Libiri perimeter of the *Société des Mines du Liptako* [67]. Also, just as in the Kplessou-Toumodi (Ivory Coast) [66], the intrusion of protolitic rocks accompanied by multiple fractures controls the arrival of hydrothermal fluids. According to the work of Nikiema [68], the hydrothermalism which allowed the remobilization and drainage of gold-rich solutions towards the fragile shear corridors (oriented NNE–SSW and NE–SW) would be synchronous with the extensive deformation phase D3. As summarized by *Placer Dome Inc.* [31], this phase could be the equivalent of the P2 phase and could be interpreted the phase that exerted structural control over gold mineralizations at the level of the Samira sedimentary horizon.

The evolution of the mineral phases shows that the association of minerals accompanying gold in the study area differs from the results obtained in certain non-orogenic West African deposits, in which gold is associated with carbonates [69], skarns [70] or copper porphyries [71]. Several works [65] [72] [73] [74] have demonstrated that orogenic deposits mainly form at the boundaries of tectonic plates and are linked to periods of crustal growth marked by intense magmatic activity conducive to the circulation of fluids. Thus, orogenic deposits would be linked to shear corridors and the commonly accepted genesis model is that of a continuum of fluid circulations from the ductile stage to the brittle stage [6]. For Groves *et al.* [73], the mineralizations would form after the peak of metamorphism, subsequent to the compressive deformation phase. Then, the presence of metamorphic minerals (chlorite and epidote; **Figure 6(f)**) reflects that gold mineralization affects supra-crustal terrains metamorphosed in green schist to amphibolite facies [6] [73].

Here we find the context of a certain mineral paragenesis associated with gold and the nature of the surrounding areas which indicate that there were at least two hydrothermal phases of establishment of gold mineralization. On the basis of a report on the exploratory petrography of Samira, the first phase is of synsedimentary exhalative origin and, during which, disseminated gold was emplaced in the metasediments [75]. The second phase has been evoked by [30], who concluded and emphased that it has a hydrothermal or late-orogenic character and is distinguished by and through the sulphurous minerals in the gray quartz veins and volcanics. In summary, the results obtained from this study are consistent with typical first phase gold mineralization, but comparison with more outcrops, drill core and face samples from an operating underground mine should be sought. Also, it is accepted that the supergene alteration of the base shear zones obviously favors a certain redistribution of gold contents [76]. Therefore, the relationship between the indices of gold mineralization, thermotectonic phenomena and the rocks carrying this mineralization could certainly be constrained by the study of concentrations [77], but additional information would be required using isotopic data (e.g. Pb, Sr and Sm-Nd).

6. Conclusion

The Société des Mines du Liptako (SML) has been operating an open-pit gold mine since 2004. Since 2016, faced with a problem of depletion of reserves, this company has been looking for new deposits in order to maintain the level of production. Thus, at the level of the "Samira Sedimentary Sequence", a RC drilling campaign over the entire eastern Boulon Djounga prospect made it possible to rely on numerous cuttings to ensure the lateral continuity and the structural context of the lithologies in depth. In order to fully exploit the use of cuttings as a tool and medium for providing information on gold grades in reserved areas, this study focused on the devices and mechanisms governing the style of mineralization and the characteristics of gold in the Sirba greenstone belt. For this, after a description of the samples of cuttings taken, thin sections were made for microscopic observations. And, to design strings (or mineralized envelopes), metallurgical operations (or chemical analyses) made it possible to determine the gold content in ppm for each representative sample of a pass. The petrographic analysis demonstrated that the eastern perimeter of Boulon Djounga corresponds to a succession of metabasalts intercalated with fragmentary metasediments, then laminated, granoclassified and interstratified, in addition to intrusions of quartz and dolerites. These lithologies are covered by ferruginous and argillaceous sandstones and spotted clays. The observation of symptomatic minerals of low pressure and low temperature such as epidote, chlorite, sericite show that the metamorphism which prevailed within the study area is the green schist facies, sometimes reaching amphibolite facies due to the presence of hornblende. The gold mineralizations are disseminated or concentrated and are hosted in metasediments, gray quartz veins or metabasalts. The importance of the lithological control of gold by the metasediments could be explained by the fact that the metabasalts of the top and base played a barrier role during the ascent of gold-rich hydrothermal fluids. This circulation of fluids would have caused the establishment of quartz with gold and sulphides, and the pseudomorphosis of primary minerals (plagioclase, pyroxene) into secondary minerals (sericite, chlorite, epidote). It is imperative that future studies combine sampling at the working face with a more rigorous evaluation of the effect of particle aggradation events in alteration corridors, particularly at the level of vein walls (quartz, dolerites and pegmatites) which are determinants of high gold concentrations in surface and in the underground conditions. After all, RC drilling techniques could well be combined with logging and isotopic data to even better ensure lateral continuity and the context of the lithologies carrying gold mineralization deeply.

Acknowledgements

We are grateful to the Director of la *Société des Mines du Liptako* (SML) and the Head of the Department of Geology, Exploration and Resource Development of SML for enabling and authorizing access to the cutting samples and chemical data.

Conflicts of Interest

The authors declare no conflicts of interest regarding the publication of this paper.

References

[1] Milési, J.P., Ledru, P., Feybesse, J., Dommanget, A., Marcoux, E. and Codex, O. (1992) Early Proterozoic Ore Deposits and Tectonics of the Birimian Orogenic Belt, West Africa. *Precambrian Research*, **58**, 305-344. https://doi.org/10.1016/0301-9268(92)90123-6

[2] Béziat, D., Dubois, M., Debat, P., Nikie, S., Salvi, S. and Tollon, F. (2008) Gold Metallogeny in the Birimian Craton of Burkina Faso (West Africa). *Journal of African Earth Sciences*, **50**, 215-233. https://doi.org/10.1016/j.jafrearsci.2007.09.017

[3] Markwitz, V., Hein, K.A.A. and Miller, J. (2016) Compilation of West African Mineral Deposits : Spatial Distribution and Mineral Endowment. *Precambrian Research*, **274**, 61-81. https://doi.org/10.1016/j.precamres.2015.05.028

[4] Goldfarb, R.J. and André-Mayer, A.S. (2017) West Africa Gold Preface. *Economic Geology*, **112**, 1-2. https://doi.org/10.2113/econgeo.112.1.1

[5] Grenholm, M., Jessell, M. and Thébaud, N. (2018) A Geodynamic Model for the Paleoproterozoic (ca. 2.27-1.96 Ga) Birimian Orogen of the Southern West African Craton-Insights into an Evolving Accretionary-Collisional Orogenic System. *Earth-Science Reviews*, **192**, 138-193. https://doi.org/10.1016/j.earscirev.2019.02.006

[6] Traoré, D.Y. (2017) Étude métallogénique du district aurifère de Syama (Mali): Analyse comparative de gisements situés sur une même structure lithosphérique éburnéenne. Ph.D. Thesis, Université de Toulouse, Toulouse.

[7] Castaing, C., Billa, M., Milesi, J.P., Thiéblemont, D., Le Metour, J., Egal, E., Donzeau, M., Guerrot, C., Cocherie, C., Chevremont, P., Tegyey, M., Itard, Y., Zida, B., Ouedraogo, I, Kote, S., Kabore, B.E., Ki, J.C. and Zunino, C. (2003) Notice explicative de la carte géologique et minière au 1/1 000 000^e du Burkina Faso. Edition du BRGM, Paris.

[8] Klemd, R. and Ott, S. (1997) Compositional Characteristics of Fluid Inclusions as

Exploration Tool for Au-Mineralization at Larafella, Burkina Faso. *Journal of Geochemical Exploration*, **59**, 251-258. https://doi.org/10.1016/S0375-6742(97)00012-5

[9] Klemd, R., Hunken, U. and Olesh, M. (2002) Metamorphism of the Country Rocks Hosting Gold—Sulfide-Bearing Quartz Veins in the Paleoproterozoic Southern Kibi-Winneba Belt (SE-Ghana). *Journal of African Earth Sciences*, **35**, 199-211. https://doi.org/10.1016/S0899-5362(02)00122-7

[10] Perrouty, S. (2012) Évolution structurale de la ceinture minéralisée d'Ashanti, SO Ghana. Ph.D. Thesis, Université de Toulouse III-Paul Sabatier, Toulouse.

[11] White, A., Burgess, R., Charnley, N., Selby, D., Whitehouse, M., Robb, L. and Waters, D. (2014) Constraints on the Timing of Late-Eburnean Metamorphism, Gold Mineralisation and Regional Exhumation at Damang Mine, Ghana. *Society of Economic Geologists*, **1**, 1009-1025. https://doi.org/10.1016/j.precamres.2013.12.024

[12] Augustin, J. (2017) Étude des minéralisations aurifères du district de Mana, Burkina Faso. Évolution hydrothermale d'un système aurifère et contraintes tectono-métamorphiques. Ph.D. Thesis, Université du Québec à Chitoutimi, Chicoutimi.

[13] Sangaré, A., Driouch, Y., Salvi, S. and Al, E. (2014) Geology of Kalana late-Eburnean Gold Deposit (Birimian, Southwestern Mali). *Bulletin de l'institut Scientifique: Rabat, Section Sciences de la Terre*, **1**, 85-108.

[14] Ballo, I., Hein, K.A.A., Guindo, B., Sanogo, L., Ouologuem, Y., Daou, G. and Traore, A. (2015) The Syama and Tabakoroni Gold Fields, Mali. *Ore Geology Reviews*, **78**, 578-585. https://doi.org/10.1016/j.oregeorev.2015.10.019

[15] Dabo, M. (2011) Tectonique et minéralisations aurifères dans les formations birimiennes de Frandi-Boboti, boutonnière de Kédougou-Kéniéba, Sénégal. Ph.D. Thesis, Université de Rennes 1, Rennes.

[16] Coulibaly, Y., Boiron, M.C., Cathelineau, M. and Kouamelan, A. (2008) Fluid Immiscibility and Gold Deposition in the Birimian Quartz' Veins of the Angovia Deposit (Yaoure, Côte d'Ivoire). *Journal of African Earth Sciences*, **50**, 234-254. https://doi.org/10.1016/j.jafrearsci.2007.09.014

[17] Koffi, A.Y., Thébaud, N., Kouamelan, A.N., Baratoux, L., Bruguier, O., Vanderhaeghe, O., Pitra, P., Kemp, A.I.S. and Evans, N.J. (2022) Archean to Paleoproterozoic Crustal Evolution in the Sassandra-Cavally Domain (Côte d'Ivoire, West Africa): Insights from Hf and U-Pb Zircon Analyses. *Precambrian Research*, **382**, Article ID: 106875. https://doi.org/10.1016/j.precamres.2022.106875

[18] Tuduri, J. (2005) Processus de formation et relations spatio-temporelles des minéralisations à or et argent en contexte volcanique. Implications sur les relations déformation-magmatisme-volcanisme-hydrothermalisme. Ph.D. Thesis, Université d'Orléans, Orléans.

[19] Pelleter, E. (2007) Géologie, géochimie et géochronologie du gisement aurifère de Tamlalt-Menhouhou (Haut-Atlas oriental). Contribution des événements Ediacariens, Ordoviciens supérieurs et Stéphano-autuniens au polyphasage des minéralisations et à la géodynamique de la Bor. Ph.D. Thesis, Institut National Polytechnique de Loraine, Nancy.

[20] Pigois, J., David, I.G., Fletcher, I.R., Mcnaughton, N.J. and Snee, L.W. (2003) Age Constraints on Tarkwaian Palaeoplacer and Lode-Gold Formation in the Tarkwa-Damang District, SW Ghana. *Mineralium Deposita*, **38**, 695-714. https://doi.org/10.1007/s00126-003-0360-5

[21] Kolb, J., Meyer, F.M., Vennemann, T., Hoffbauer, R., Gerdes, A., Sakellaris, G.A., Kolb, J., Meyer, F.M., Vennemann, T., Hoffbauer, R., Gerdes, A. and Sakellaris, G.A. (2008) Geological Setting of the Guelb Moghrein Fe Oxide-Cu-Au-Co Mineraliza-

tion, Akjoujt Area, Mauritania. *Geological Society of London*, **297**, 53-75. https://doi.org/10.1144/SP297.4

[22] Béziat, D., Siebenaller, L., Salvi, S. and Chevalier, P. (2016) A Weathered Skarn-Type Mineralization in Ivory Coast: The Ity Gold Deposit. *Ore Geology Reviews*, **78**, 724-730. https://doi.org/10.1016/j.oregeorev.2015.07.011

[23] Bamba, O., Parisot, J.C., Grandin, G. and Beauvais, A. (2002) Ferricrete Genesis and Supergene Gold Behavior in Burkina Faso, West Africa. *Geochemistry: Exploration, Environment, Analysis*, **2**, 3-14. https://doi.org/10.1144/1467-787302-001

[24] Le Mignot, E., Siebenaller, L., Béziat, D., Reisberg, L., Salvi, S., Velasquez, G., Zimmermann, C., Naré, A., Franceschi, G. and Nancy, F.-V. (2017) The Paleoproterozoic Copper-Gold Deposits of the Gaoua District, Burkina Faso : Superposition of Orogenic Gold on a Porphyry Copper Occurrence ? *Society of Economic Geologists*, **112**, 99-122. https://doi.org/10.2113/econgeo.112.1.99

[25] Markwitz, V., Hein, K.A.A., Jessel, M.W. and Miller, J. (2016) Metallogenic Porfolio of the West Africa Craton. *Ore Geology Reviews*, **78**, 558-563. https://doi.org/10.1016/j.oregeorev.2015.10.024

[26] Masurel, Q., Thébaud, N., Miller, J., Ulrich, S., Hein, K.A.A., Cameron, G., Béziat, D., Bruguier, O. and Davis, J.A. (2017) Sadiola Hill: A World-Class Carbonate-Hosted Gold Deposit in Mali, West Africa. *Society of Economic Geologists*, **112**, 23-47. https://doi.org/10.2113/econgeo.112.1.23

[27] Machens, E. (1961) Prospection générale du Liptako. République du Niger. Ministère Des Travaux Publics et Des Mines. BRGM, Niamey.

[28] Machens, E. (1973) Contribution à l'étude des formations du socle cristallin et de la couverture sédimentaire de l'Ouest de la République du Niger. Mémoire du BRGM, Paris.

[29] Hamilton, J. (1996) Notes on the Geology of the Samira and Boulon Djounga Deposit Areas, Libiri NW, Tiawa Concession, Southwestern Niger. Report for Etruscan Enterprises, Kingman.

[30] Placer Dome Inc. (1997) Samira and Taghlit Projects, Aribas, A. Visit Report october 8. Placer Dome Exploration Inc., Vancouver.

[31] Placer Dome Inc. (1997) Summary notes on the Geological Modelling of the Samira Deposit, Tiawa Concession, Niger. Norman Jun 1997 Report, Placer Dome Exploration Inc., Vancouver.

[32] SML (2008) Étude de faisabilité du gisement d'or de Boulon Djounga. SML Niger, Niamey.

[33] SML (2016) Rapport du développement de gisement d'or de Boulon Djounga Est. SML Niger, Niamey.

[34] Milési, J.P., Feybesse, J.L., Ledru, P., Dommanget, A., Ouédraogo, M.F., Marcoux, E., Prost, A.E., Vinchon, C., Sylvain, J.P., Johan, V., Tegyey, M., Calvez, J.Y. and Lagny, P. (1989) Les minéralisations aurifères de l'Afrique de l'Ouest. Leurs relations avec l'évolution lithostructurale au Protérozoïque inférieur. *Chronique de la Recherche Minière*, **497**, 3-98.

[35] Béziat, D., Bourges, F., Debat, P., Lompo, M., Martin, F. and Tollon, F. (2000) A Paleoproterozoic Ultramafic-Mafic Assemblage and Associated Volcanic Rocks of the Boromo Greenstone Belt: Fractionates Originating from Island-Arc Volcanic Activity in the West African Craton. *Precambrian Research*, **101**, 25-47. https://doi.org/10.1016/S0301-9268(99)00085-6

[36] Ennih, N. and Liégeois, J.P. (2008) The Boundaries of the West African Craton, with Special Reference to the Basement of the Moroccan Metacratonic Anti-Atlas

Belt. *Geological Society*, **297**, 1-17. https://doi.org/10.1144/SP297.1

[37] Vidal, M., Gumiaux, C., Cagnard, F., Pouclet, A., Ouattara, G. and Pichon, M. (2009) Evolution of a Paleoproterozoic "Weak Type" Orogeny in the West African Craton (Ivory Coast). *Tectonophysics*, **477**, 145-159. https://doi.org/10.1016/j.tecto.2009.02.010

[38] Dupuis D. and Pons J.P.A. (1991) Mise en place de plutons et caractérisation de la déformation au Niger occidental. *Comptes Rendus de l'Académie des Sciences de Paris*, **323**, 769-776.

[39] Ama Salah, I., Liegeois, J.P. and Pouclet, A. (1996) Évolution d'un arc insulaire océanique birimien précoce au Liptako nigérien (Sirba): Géologie, géochronologie et géochimie. *Journal of African Earth Sciences*, **22**, 235-254. https://doi.org/10.1016/0899-5362(96)00016-4

[40] Soumaila, A. and Konaté, M. (2005) Caractérisation de la déformation dans la ceinture birimienne (paléoprotérozoique) de Diagorou-Darbani (Liptako nigérien, Afrique de l'Ouest). *Africa Geoscience Review*, **12**, 161-178.

[41] Soumaila, A., Henry, P., Garba, Z. and Rossi, M. (2008) REE Patterns, Nd-Sm and U-Pb Ages of the Metamorphic Rocks of the Diagorou-Darbani Greenstone Belt (Liptako, SW Niger): Implication for Birimian (Palaeoproterozoic) Crustal Genesis. *Geological Society*, **297**, 19-32. https://doi.org/10.1144/SP297.2

[42] Soumaila, A., Garba, Z., Moussa, I.A., Nouhou, H. and Sebag, D. (2016) Highlighting the Root of a Paleoproterozoic Oceanic arc in Liptako, Niger, West Africa. *Journal of Geology and Mining Research*, **8**, 13-27. https://doi.org/10.5897/JGMR2015.0230

[43] Soumaila, A., Ahmed, Y. and Nouhou, H. (2016) Géochimie des basites et ultrabbasites de Ladanka (Liptako, Niger). *Journal Des Sciences*, **16**, 37-54.

[44] Garba Saley, H.G., Konaté, M., Ahmed, Y. and Soumaila, A. (2017) Les minéralisations de manganèse du Nord Téra (Liptako, Ouest Niger): Origine et conditions de mise en place. *Revue Cames*, **5**, 18-28.

[45] Garba Saley, G.H., Soumaila, A. and Konaté, M. (2018) Alteration Processes of Paleoproterozoic Manganese Protores of the North Téra: Mineralogy and Geochemistry (West Africa). *Journal of Geological Resource and Engineering*, **6**, 177-193. https://doi.org/10.17265/2328-2193/2018.05.001

[46] Hallarou, M.M., Konaté, M., Olatunji, A.S., Ahmed, Y., Ajayi, F.F. and Abdul, R.M. (2020) Re-Os Ages for the Kourki Porphyry Cu-Mo Deposits, North West Niger (West Africa): Geodynamic Implications. *European Journal of Environment and Earth Sciences*, **1**, 1-13. https://doi.org/10.24018/ejgeo.2020.1.4.43

[47] Hallarou, M.M., Konaté, M., Ahmed, Y., Chékaraou, M.M.S., Attourabi, S.A., Chamsi, L.I. and Noura, G.R. (2022) Paleoproterozoic Basalt Rocks Related to Plumes in the Gorouol Belt (Liptako West Niger). *International Journal of Scientific Engineering and Applied Science*, **8**, 66-73.

[48] Ahmed, Y., Attourabi, S.A., Hallarou, M.M., Chamsi, L.I., Noura, G.R. and Sanda, C.M.M. (2023) Relationship between Regional Deformation and the Emplacement of the Dibilo Pegmatites (Liptako, West Niger). *Journal of African Earth Sciences*, **198**, Article ID: 104814. https://doi.org/10.1016/j.jafrearsci.2022.104814

[49] Lama, C. (1993) Apport de la méthode K-Ar à la compréhension de l'histoire géologique des granitoïdes birimiens du Liptako (Niger Occidental) et des leucogranites à deux micas de Tagragra d'AKKA (Anti-Atlas Occidental, Maroc). Master's Thesis, Université de Loraine, Nancy.

[50] Pons, J., Barbey, P., Dupuis, D. and Léger, J.M. (1995) Mechanisms of Pluton Emplacement and Structural Evolution of a 2.1 Ga Juvenile Continental Crust: The Bi-

rimian of Southwestern Niger. *Precambrian Research*, **70**, 281-301.
https://doi.org/10.1016/0301-9268(94)00048-V

[51] Abdou A., Bonnot H., Bory Kadey D., Chalamet D., Saint Martin, M. and Younfa, I. (1998) Notice explicative des cartes géologiques du liptako à 1/100000e et 1/200 000e. Ministère Des Mines et de la Géologie, République du Niger, Niamey, 64.

[52] Konaté, M., Ahmed, Y., Gärtner, A.D., Alzouma, A.H., Ibrahim, M., Tourba, K., Hofmann, M., Zieger, J. and Linnemann, U. (2018) U-Pb Detrital Zircon Ages of Sediments from the Firgoun and Niamey Areas (Eastern Border of West African Craton, West Niger). *Comptes Rendus Geoscience*, **350**, 267-278.
https://doi.org/10.1016/j.crte.2018.06.005

[53] Ibrahim Maharou, H. (2020) Dynamique sédimentaire des grès de Niamey (Niger occidental): Indices de glaciation et déformations associées. Ph.D. Thesis, Université Abdou Moumouni, Niamey.

[54] Alzouma, G., Konaté, M. and Ahmed, Y. (2020) Geodynamic Context of the Proterozoïc Deposits of the Firgoun Region (Eastern Border of the West African Craton, West Niger). *Geological Society of London*, **502**, 215-236.
https://doi.org/10.1144/SP502-2019-115

[55] Ousmane, H., Hantchi, K.D., Hamidou, L.B., Ali, I.A. and Konaté, M. (2020) Caractérisation de la déformation des dépôts oligocènes du Continental terminal 3 (Ct3) dans la région de Niamey (Bordure Orientale du Craton Ouest Africain, Bassin des Iullemmeden). *European Scientific Journal*, **16**, 418-441.
https://doi.org/10.19044/esj.2020.v16n15p418

[56] Ouattara, Z., Emmanuel Gouedji, G.F., Beugre Dago, A.G., Koffi, A.A.F., Allialy Marc Ephrem, A.M. and Coulibaly, Y. (2022) The Hydrothermal Alteration Activity Related to the Orogenic Lode-Gold at Kplessou, Toumodi, Côte d'Ivoire. *Earth Sciences*, **11**, 356-363.

[57] Ama Salah, I. (1991) Pétrographie et relations structurales des formations metavolcaniques et sédimentaires du Birimien du Niger occidental. Problème de l'accrétion crustale au paléoprotérozoique inférieur. Ph.D. Thesis, Université d'Orléans, Orléans.

[58] Gaboury, D. (2009) Rapport de visites géologiques, SML Niger, Niamey.

[59] Gaboury, D. (2019) Les minéralisations aurifères d'Afrique de l'Ouest: Différences et similitudes avec l'Abitibi. Technical Report. *Ressources Mines et Industrie*, *6*, 37-42.

[60] Eggleton, R.A. (2001) The Regolith Glossary, Surficial Geology, Soils and Landscapes. Copyright Cooperative Research Centre for Lanscape Evolution and Mineral Exploration and CSIRO Exploration and Mining, Canberra.

[61] Gilders, R. (1999) Petrographic Report on Samira Hill Core Samples. Visit Report Prepared for Etruscan Enterprises, Kingman.

[62] Leube, A., Hirdes, W., Mauer, R. and Kesse, G.O. (1990) The Early Proterozoic Birimian Supergroup of Ghana and Some Aspects of Its Associated Gold Mineralization. *Precambrian Research*, **46**, 139-165.
https://doi.org/10.1016/0301-9268(90)90070-7

[63] Oberthur, T., Vetter, U., Mumm, A.S., Weiser, T., Amanor, J.A., Gyapong, W.A., Kumi, R. and Blenkinsop, T.G. (1994) The Ashanti Gold Mine at Obuasi, Ghana: Mineralogical, Geochemical, Stable Isotope and fluid Inclusion Studies on the Metallogenesis of the Deposit. *Geologisches Jahrbuch*, **D100**, 31-129.

[64] Mcmahon, G., Oberthur, T., Cabri, L.J., Weisner, T.W., McMahon, G. and Muller, P. (1997) Pt, Pd and Other Trace Elements in Sulfides of the Main Sulfide Zone, Great Dyke, Zimbabwe: A Reconnaissance Study. *Canadian Mineralogist*, **35**, 597-609.

[65] El-Desoky, H.M., Shahin, T.M.m Yahia, Z. and Amer, Y.Z. (2021) Characteristic of Gold Mineralization Associated with Granites at Hamash Old Gold Mine, South Eastern Desert, Egypt. *Arabian Journal of Geosciences*, **14**, Article No. 558. https://doi.org/10.1007/s12517-021-06923-9

[66] Ouattara, Z. Gouedji, G.F.E., Beugre Dago, A.G., Koffi, A.A.F., Allialy Marc Ephrem, E.M. and Coulibaly, Y. (2022) The Hydrothermal Alteration Activity Related to the Orogenic Lode-Gold at Kplessou, Toumodi, Côte d'Ivoire. *Earth Sciences*, **11**, 356-363.

[67] Sidi, A.A.M. (2014) Rôle de la déformation dans la mise en place de la minéralisation aurifère dans le permis de Samira/Libiri: cas du gisement de Libiri. Master's Thesis, Université Abdou Moumouni, Niamey.

[68] Nikiema, S. (1992) Contexte structurale et implication métallogéniques au sein du permis de "ESSEKANE" dans le sillon de Dori. Géométrie des corps aurifères, Essakane Gold Mine, Burkina Faso, Orezone Resources and IAMGOLD (Toronto, Ontario, Canada).

[69] Oberthur, T., Schmidt, M.A., Vetter, U., Simon, K. and Amanor, J.A. (1996) Gold Mineralization in the Ashanti Belt of Ghana: Genetic Constraints of the Stable Isotope Geochemistry. *Economic Geology*, **91**, 289-301. https://doi.org/10.2113/gsecongeo.91.2.289

[70] Lawrence, D.M., Allibone, A.H., Chang Z., Meffre S., Lambert-Smith J.S. and Treloar, P.J. (2017) The Tongon Au Deposit, Northern Côte d'Ivoire: An Example of Birimian Au Skarn Mineralization. *Economic Geology*, **112**, 1571-1593.

[71] Kazapoe, R.W. (2023) A Review of the Characteristics and Geological Settings of Orogenic Gold Deposits of the Boule Mossi Domain: Implication for Gold Exploration. In. Geology, Ecology, and Landscapes, Taylor & Francis Group, 16 p. https://doi.org/10.1080/24749508.2023.2256553

[72] Goldfarb, R.J., Groves, D.I. and Gardoll, S. (2001) Orogenic Gold and Geologic Time : A Global Synthesis. *Ore Geology Reviews*, **18**, 1-75. https://doi.org/10.1016/S0169-1368(01)00016-6

[73] Groves, D.I. (2003) Gold Deposits in Metamorphic Belts: Overview of Current Understanding, Outstanding Problems, Future Research, and Exploration Significance. *Economic Geology*, **98**, 1-29.

[74] Kamar, M.S. (2020) New Occurrence of Gold Mineralization at the Eastern Part of Wadi El Gemal, South Eastern Desert, Egypt. *Open Journal of Geology*, **10**, 1210-1233. https://doi.org/10.4236/ojg.2020.1012060

[75] Klipfel, P. (1997) Petrographic Report, Samira Project. Report Prepared for Placer Dome Exploration Inc, Vancouver.

[76] Boubacar Abdou, F. (2023) Apport de la télédétection et du SIG dans la cartographie des zones minéralisées: Secteurs du Sud Maradi et du Damagaram-Monio (Sud-Est Niger). Ph.D. Thesis, Université Abdou Moumouni, Niamey.

[77] Gnamou, B., Ilboudo, H., Toé, W.A.B. and Sawadogo, S. (2023) Geochemical Mobility Associated to Gold and Base Metal Occurrences of Mangodara Sector, in Southern Burkina Faso, Banfora Greenstone Belts (West African Craton). *Open Journal of Geology*, **13**, 1024-1053. https://doi.org/10.4236/ojg.2023.1310044